Int. J. Electrochem. Sci., 16 **(2021)** Article Number: 211250, doi: 10.20964/2021.12.29

International Journal of
ELECTROCHEMICAL
SCIENCE
www.electrochemsci.org

Research on Stray Current Distribution in a Multitrain Subway System using Finite Element Modeling

Shan Lin[1], *Xuehua Liu*[2], *Xianwei Zhang*[2], *Zhichao Cai*[2,*]

[1] Guangzhou Metro Design&Research Institute Co.,Ltd, Guangzhou 510010, China.
[2] School of Electrical and Automation Engineering, East China Jiaotong University, Nanchang 330013, China.
[*]E-mail: czchebut@foxmail.com

Received: 28 June 2021 / *Accepted:* 30 September 2021 / *Published:* 10 November 2021

Stray current modeling analysis is an important method to study the leakage and distribution of stray current. To study the stray current distribution law under the combined influence of multiple trains in the up and down subway section, this paper takes the interference of stray current on buried pipelines as the research object and establishes a field-circuit coupling model combining a resistor network model with an electric field model. This paper focuses on the analysis of the distribution of stray current in the soil environment under the condition of multiple trains in up and down section, the change of buried pipeline current and pipe-ground potential under the interference of stray current, the drainage efficiency of a drainage network under different settings, and the protection efficiency of a pipeline anti-corrosion layer against stray current. The simulation results show that the leakage of stray current in the soil is not determined by the number of trains on the line but by the average traction current of the train. The simulation results also show that the drainage effect of the drainage network depends on the longitudinal cross-sectional area of the drainage network. When both the track bed reinforcement and the tunnel structure reinforcement participate in drainage, the efficiency of the drainage network is as high as 81.1%. The protection efficiency of the anti-corrosive layer against stray current is over 90%. The new field-circuit coupling model combines the computational advantages of resistance and the finite element method and provides a new idea for solving the modeling and analysis of stray currents in complex environments.

Keywords: stray current, field-circuit coupling, buried pipeline, drainage network, anti-corrosion layer

1. INTRODUCTION

DC power supplies are generally used in urban rail transit, and rails are often used as the return path of traction current. Due to the existence of rail self-resistance and the inability to achieve complete insulation between the rail and the ground, part of the traction current will leak to the ground and form a stray current [1]. A large amount of stray current leakage to the ground will cause the electrochemical

corrosion of buried metals [2,3], which will seriously endanger the safety of workers and trackside equipment [4]. Worldwide, scholars have focused on stray current modeling and analysis [5-12], stray current corrosion law research [13], stray current corrosion prediction [14,15] and stray current leakage monitoring [16]. The research results have been widely applied to the stray current prevention of urban rail transit.

Modeling analysis is not only the most commonly used means to study the distribution of stray current but is also the basis of stray current monitoring and detection. For example, in terms of the resistance model, Mccollum [5] established a rail-earth resistance model as early as the beginning of the 21st century and proposed the concept of the leakage rate of stray current for the first time, which provides an evaluation method for the evaluation of stray current. The resistance model proposed by Ogunsola [8] fully considers the influence of train characteristics, train interval time, multitrain movement and other factors on the stray current. The resistance model is simple to build and convenient to calculate, but there are many idealized assumptions, which are not applicable to all situations.

In recent years, new methods and simulation software have been continuously applied to the modeling of stray currents. For example, Hu [9] established a three-dimensional finite element model of a stray current field by using the finite element method (FEM) and analyzed the distribution law of stray current and potential in the solution domain. Yi [10] established a three-dimensional model of stray current distribution for reinforced concrete bridges by using the boundary element method (BEM) and analyzed the law of corrosion of the steel anode area of bridge structures changing with the applied voltage. Bortels [11] established a stray current model coupled with finite elements and boundary elements based on the advantages of the finite element method and boundary element method. The above models enrich the types of stray current models but also have their own limitations. For example, the calculation efficiency of the finite element model is relatively low. Although the boundary element method improves the computational efficiency, it does so at the cost of ignoring the details in the solution domain. Therefore, establishing a model that can reflect the characteristics of complex environments and accurately analyze the distribution law of stray currents in a specific area is particularly important.

At present, stray current research modeling at home and abroad is built around the single-track operation of trains. For example, Liu [17] studied the measurement of track transition resistance under a single train and Wang [18] studied the distribution of stray current under the long line of urban rail transit, but they all ignored that in the fact that actual subway trains run in both directions according to the operation diagram (timetable). Therefore, there will be a great deviation in the solution of stray current. Based on the above problems, this paper established a field-circuit coupling model combining a resistance network model and an electric field model for the first time. Good conductors such as rail and drainage networks are selectively replaced by resistance, and the soil area and buried pipeline are calculated by the finite element method; thus, the calculation and research of stray current distribution under the dynamic condition of up and down multiple trains are realized.

2. URBAN RAIL TRANSIT POWER SYSTEM AND OPERATION LAW OF INTERVAL TRAINS

As shown in Fig. 1, the metro main substation first stepped down the 110 kV AC power of the

urban power grid to 35 kV AC, and then the 35 kV AC power was stepped down and rectified at the metro traction substation to convert it to DC 1500 V, which was used as the rated voltage to supply electric power to the traction train. The current circulation path of the metro DC part is as follows: traction substation - up and down overhead contact network - interval train - return system (including rail, return current sharing cable, drainage network, ground network, etc.) - traction substation.

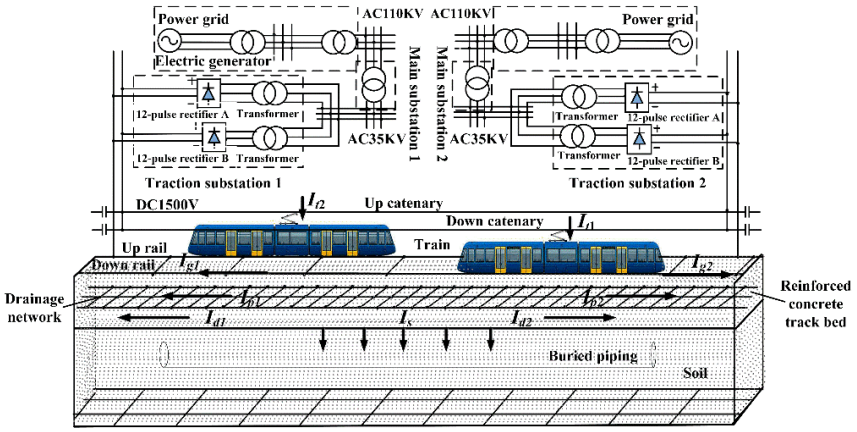

Figure 1. Schematic diagram of stray current leakage in a subway bilateral power supply system

The train operation schedule [17] of the Guangzhou Metro Line 2 phase 1 project is shown in Fig. 2. There are 10 stations on the line, of which 5 are traction substation stations and the other 5 are nontraction substation stations. At 40 s, the up and down trains depart from station 10 and station 1 in the opposite direction. When all the trains are out, the trains on the interval show periodic regularity. Fig. 3(a) shows the curves of the trains passing through the up and down section of Station 1 and Station 3 between 850 s and 1200 s (including a stable period) and their corresponding traction currents. During this period, the up trains are B1 and B2, and the down trains are A5, A6 and A7. Assuming that the traction current of each train passing through Station 1 and Station 3 remains unchanged, as shown in Fig. 3(b), the traction current curve of train A6 passes through Station 1 and Station 3 (the data are taken from the TDS field collection data of CSR Zhuzhou Electric Locomotive Research Institute).

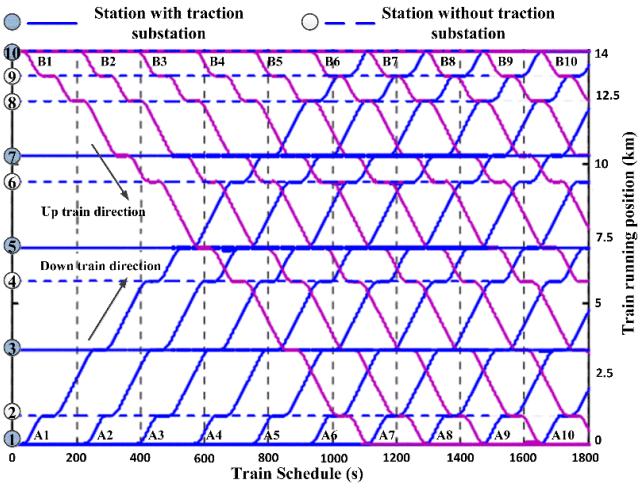

Figure 2. Interval train timetable

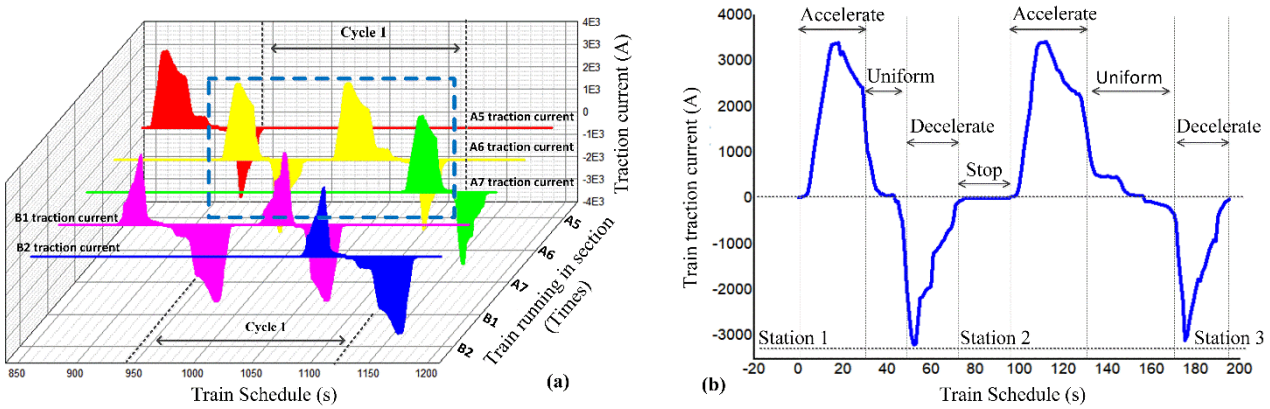

Figure 3. Time-traction current curve of interval train operation: (a) train and traction current between station 1 and station 3, and (b) A6 traction current.

3. STRAY CURRENT LEAKAGE MODEL ESTABLISHMENT AND DESCRIPTION

The DC traction power supply system returns directly through the rail, sets the current sharing line between the same track rail (interval of 200 m~300 m) and between the up and down rails (interval of 500 m~600 m), and shorts four rails up and down to reduce the loop impedance [19]. In the subway system, the drainage network is located directly below the rail and is composed of longitudinal drainage strips welded with transverse reinforcement; Among them, the longitudinal drainage strip is connected by transverse reinforcement to form a parallel structure[18]. Reinforced concrete track bed steel bars and tunnel steel bars are usually set as drainage networks [20-21] to realize the collection of stray current and reduce leakage. This paper builds a stray current model to observe the influence of stray current in the soil on buried pipelines. In Fig. 1, the steel rail and the drainage network have good electrical conductivity and can be directly equivalent to a resistance as a part of the circuit; traction substation 1 and traction substation 2 together provide traction current for the interval trains. According to Fig. 1, a model combining the circuit and electric field is established. A schematic diagram of the newly established model is shown in Fig. 4. Train 1 provides current for the model, and the resistances of the rail, track bed and drainage network on the left and right sides of train position L1 are represented by R_{g1}, R_{g2}, R_{d1}, R_{d2}, R_{p1} and R_{p2}, respectively.

Taking train 1 as an example, its traction current is I_{t1}. After passing through the train, I_{t1} is divided into two parts: I_{g1} and I_{g2}, which mainly return to the left and right traction substations through the rails (R_{g1} and R_{g2}). At the same time, the current flowing into the reinforced concrete track bed is divided into I_{d1} and I_{d2} to return to the traction substation. If the drainage network is put into operation, the currents I_{p1} and I_{p2} absorbed by the drainage network will be returned to the traction substation through the drainage network. When there is only one train in the interval (train 1), according to Kirchhoff's current law, the stray current I_{S1} leaking into the soil can be expressed by equation (1):

$$I_{S1} = I_{t1} - I_{g1} - I_{g2} - I_{d1} - I_{d2} - I_{p1} - I_{p2} \quad (1)$$

The conductor resistivity is ρ, the cross-sectional area is S, and the length is L. According to equation

(2), the resistance R of conductors such as rails, drainage networks and track beds can be obtained.

$$R = \frac{\rho L}{S} \tag{2}$$

If there are N trains on the subway power supply interval at the same time, then the stray current interference of the buried pipeline in the soil field is the result of the combined action of N trains.

$$I_S = \sum_{1}^{N} I_{SN} \tag{3}$$

The distribution of stray current in the soil and its influence on buried pipelines can be solved and analyzed by the finite element method based on constant electric field theory. Fig. 5 shows the two-dimensional geometry and grid division of the soil field of the buried pipeline in the interval from Guangzhou South Station (Station 1) to Huijiang Station (Station 3) of Guangzhou Metro. The whole site is 3.37 kilometers from Guangzhou South Station to Huijiang Station, and the interval between the two stations is simplified into a rectangle of 3370×200 m^2, as shown in Fig. 5(a). In Fig. 5(a), the upper blue border is the contact surface between the soil and reinforced concrete track bed, that is, the leakage surface of stray current; the two ends of the blue border on the side represent the grounding electrode of the traction substation; and the lower green border represents the ground network. A buried pipeline (black) with a length of 3000 m and a diameter of 2 m is set in the soil, with a buried depth of 50 m.

This paper focuses on the impact of stray current leakage into the soil on buried pipelines. Considering that the distribution of stray current in the soil is a constant electric field problem, this is solved by the finite element method. COMSOL Multiphysics® is a powerful multiphysical field simulation software that can solve Maxwell's equations by using the "AC/DC Module". The governing equation is:

$$\begin{aligned} \nabla \times \boldsymbol{E} &= 0 \\ \nabla \times \boldsymbol{J} &= 0 \end{aligned} \tag{4}$$

where $\boldsymbol{E}$ is the intensity of the electric field and $\boldsymbol{J}$ is the surface density of the current.

According to the calculation requirements of the finite element method, the soil area and the buried pipeline are meshed, and the meshing result is shown in Fig. 5(b). Fig. 5(c) shows the boundary conditions of the solution field. The blue boundary represents the field insulation boundary, that is, the current in the field will not flow out of the boundary, which can be expressed by equation (4):

$$\mathbf{n} \cdot \boldsymbol{J} = 0 \tag{5}$$

where **n** is the unit normal vector.

The voltage V of the grounding part (green area) of the field is assigned to 0 V. According to the theory of a constant electric field, the current area density $\boldsymbol{J}$ at each position in the field can be obtained according to Ohm's law:

$$\boldsymbol{J} = \sigma \boldsymbol{E} \tag{6}$$

where σ represents the electrical conductivity of the medium (soil, buried pipe, and pipe insulation layer) in the domain.

The total stray current I_S (equation 3) flowing into the field is determined by the number of up and down trains in the interval. According to the current conservation law, I_S can be expressed as the area fraction of current density $\boldsymbol{J}$ flowing into the soil surface S:

$$I_S = \int_S \boldsymbol{J} dS \tag{7}$$

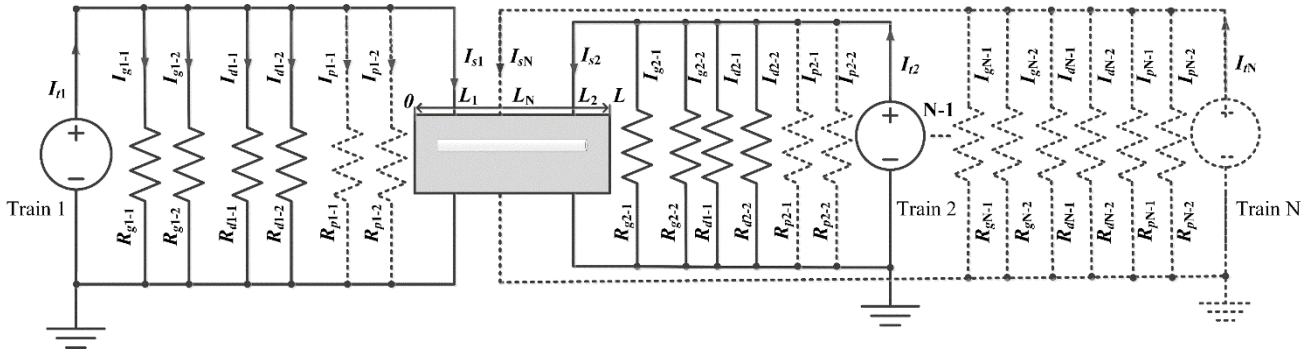

Figure 4. Schematic diagram of the field-circuit coupling model

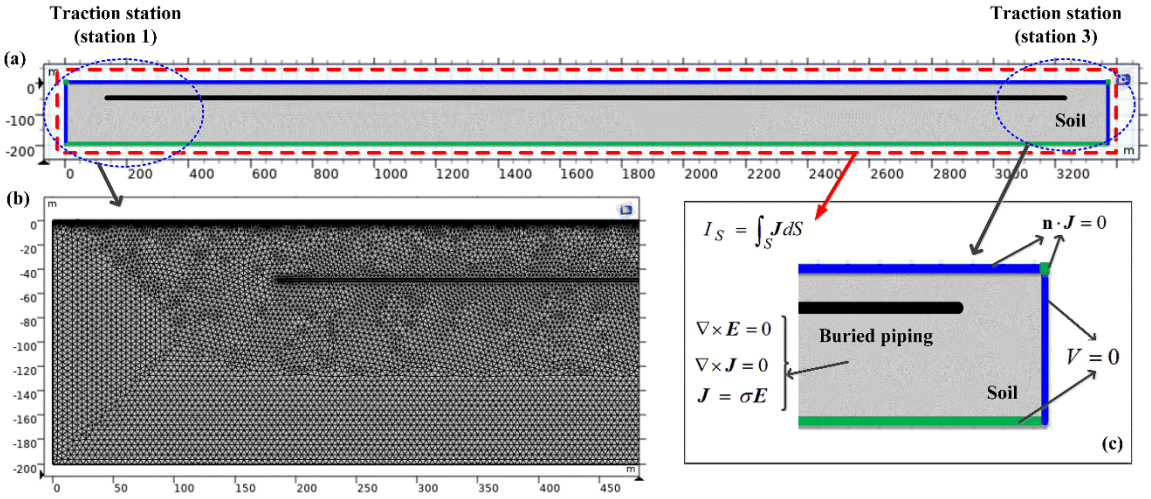

Figure 5. The geometry and boundary conditions of the electric field model: (a) model, (b) grid division, and (c) boundary.

4. ANALYSIS OF SIMULATION RESULTS

The specific parameters involved in the model are shown in Table 1, and several special working conditions in Table 2 are selected for simulation analysis. Fig. 6 is the cloud diagram of the corresponding stray current distribution under 7 working conditions. At working conditions 1 and 7, three trains run in the interval, and two trains run at the other time. Comparing the stray current density at several times, it can be found that when the three trains are running in the interval at the same time, the stray current density is relatively small as a whole because the average traction current of the three trains is also relatively small. When there are two trains in the interval, the stray current density in the soil is obviously larger due to the larger average traction current. For example, under working condition 1, both A6 and B1 are in the Decelerate stage, and the traction currents are -3187 A and -1716 A, respectively; under working condition 5, A6 and B1 are in the Accelerate stage at the same time, and the traction currents are 2970 A and 2011 A, respectively.

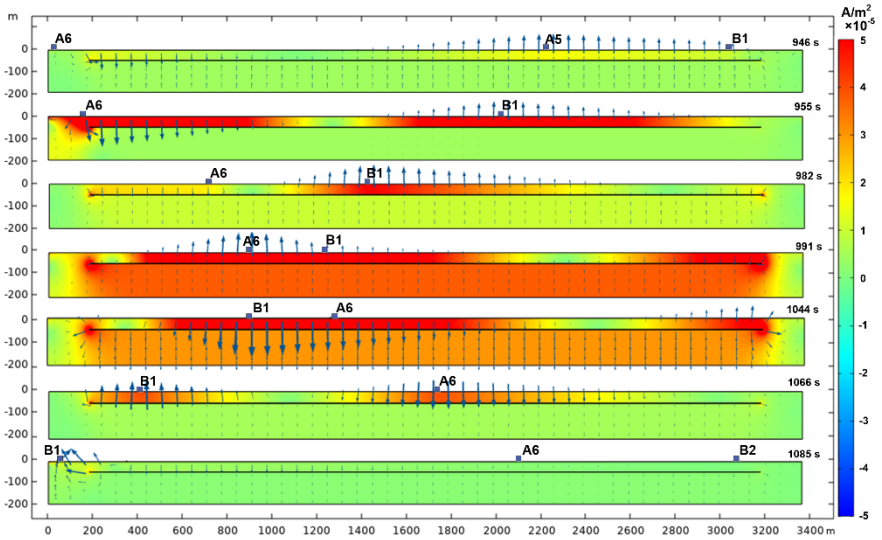

Figure 6. Cloud image of stray current distribution in the soil and buried pipeline

Fig. 6 shows that the current flow direction and size on the buried pipeline are closely related to the traction current, and the direction of the traction current determines the distribution trend of the stray current in the soil. The periodic change in traction current leads to the periodic corrosion trend of the buried pipeline. Therefore, by comparing the simulation results of several specific moments between Station 1 and Station 3, it can be concluded that the average traction current of trains in the region from 500 m to 2000 m is relatively large, and we should pay attention to this region. Du [22] divided the focus areas according to the periodic change of corrosion trend, but this paper adopts multi-train modeling, which makes the regional division more accurate and more in line with the actual situation.

Table 1. Model parameters

Model structure	Description	Value
Rail	Type	60 kg/m
	Longitudinal Section Area	77.45 cm^2
	Resistance	35 mΩ/km
Track bed	Longitudinal Section Area	10×0.5 m^2
	Resistivity	1.7e3 Ω·m
Drainage network	Reinforcement radius of ballast	8 mm
	Cross-sectional area	200.96 mm^2
	Resistivity of reinforcement in track bed	1E-7 Ω·m
	Reinforcement radius of tunnel	10 mm
	Cross sectional area	314 mm^2
	Resistivity of reinforcement in tunnel	1E-7 Ω·m
	Total	20
	Total sectional area	9495 mm^2

Soil	Conductivity Permittivity	50 Ω·m 12
Buried metal pipeline	Resistivity Permittivity	1E-7 Ω·m 1E7
3PE anticorrosive layer	Conductivity Permittivity	6.28E-5 S/m 2.3
Epoxy powder anticorrosive layer	Conductivity Permittivity	1.26E-4 S/m 3.5
Petroleum bitumen layer	Conductivity Permittivity	6.28E-4 S/m 2.5

Table 2. Working conditions

Working condition	Train	Running state	Location	Traction current
Working condition 1 (946 s)	A6	Accelerate	20 m	1086 A
	A5	Uniform	2220 m	-119 A
	B1	Decelerate	3040 m	-1015 A
Working condition 2 (955 s)	A6	Accelerate	150 m	3364 A
	B1	Decelerate	2020 m	-498 A
Working condition 3 (982 s)	A6	Uniform	710 m	71 A
	B1	Accelerate	1420 m	3344 A
Working condition 4 (991 s)	A6	Decelerate	900 m	-3187 A
	B1	Decelerate	1240 m	-1716 A
Working condition 5 (1044 s)	B1	Accelerate	890 m	2970 A
	A6	Accelerate	1260 m	2011 A
Working condition 6 (1066 s)	B1	Decelerate	410 m	-2047 A
	A6	Accelerate	1730 m	2283 A
Working condition 7 (1085 s)	B1	Decelerate	40	-1974 A
	A6	Uniform	2150	149 A
	B2	Accelerate	3080	394

5. THE INFLUENCE OF THE DRAINAGE NETWORK AND PIPELINE ANTICORROSION LAYER ON STRAY CURRENT

5.1 Setting and drainage effect of the drainage network

At present, there are many calculation formulas and simulations of subway stray current without drainage network at home and abroad, but the influence of drainage network is rarely considered [23]. In the process of metro operation, to reduce the corrosion hazard caused by stray current, a drainage

network is usually installed in the track bed to absorb and recover the leakage stray current to the negative pole of the substation. Fig. 7 and Fig. 8 are the curves of the stray current density and pipe-ground potential of the buried pipeline under 7 working conditions, respectively.

It can be seen from Fig. 7(a) and Fig. 7(b) that the distribution trend of stray current remains the same overall, but whether a drainage network is invested or not will affect the drainage effect. Under working condition 4, the maximum current density on the buried pipeline is 0.1 A/m^2 when the drainage network is not put into operation in Fig. 7(a). In Fig. 7(b), when the drainage network is put into operation, the maximum current density on the buried pipeline is 0.081 A/m^2, which decreases by 19%. The results show that the current density on the buried pipeline decreases by 18.6% and 29.5% under working conditions 5 and 6, respectively, after the drainage network is put into operation. Comparing Fig. 8(a) and Fig. 8(b), we can see that the pipe ground voltage (absolute value) before and after the discharge network is put into operation under condition 4, condition 5 and condition 6 decreases from 1.72 V to 1.31 V, 1.75 V to 1.33 V, and 0.9 V to 0.62 V, and the decline rates of the pipe ground potential are 23.8%, 24% and 31.1%, respectively. Under the condition that the longitudinal resistance of the drainage network is the same as that of the rail, the stray current flowing into the structural steel bar will be reduced by an average of 20% compared with that without the drainage network. At the same time, the above data are in good agreement with Cai's research [24]. That is, when the locomotive runs farther away from the negative pole of the traction substation, the maximum stray current density of the drainage network along the line and the potential of the pipeline to the ground along the line are greater.

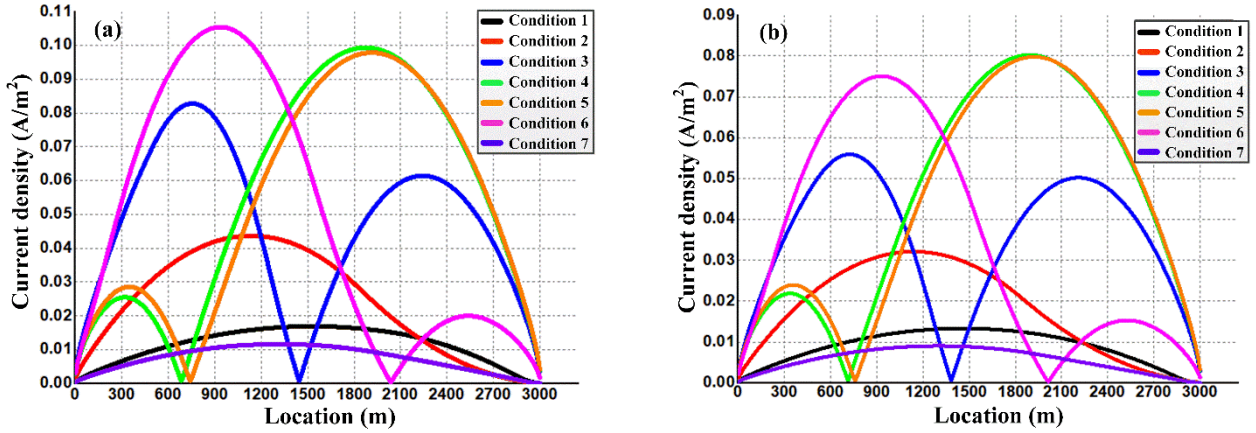

Figure 7. Current density over the length of the buried pipeline: (a) uncommitted and (b) committed

From the above conclusions, it can be seen that only the reinforced concrete structure steel bars participate in drainage, and the drainage effect is not obvious. Jin [25] introduced the longitudinal reinforcement of the concrete track bed on the tunnel wall into the drainage network, and the drainage effect was greatly improved. In the simulation, the number of longitudinal reinforcements of the reinforced concrete track bed is increased to 32, and the structural steel bar of the tunnel wall concrete is put into use as a drainage network. The longitudinal cross-sectional area of the drainage network is changed from 3215 mm^2 to 12713 mm^2. The simulation results show that after increasing the cross-sectional area of the drainage network, the stray current density on the buried pipeline decreases by 75.8%, 69.2% and 81.1% at working conditions 4, 5 and 6, respectively. The corresponding pipe-to-ground potential dropped by 76.2%, 79.7% and 85.3%, respectively.

From the above simulation comparison, it can be seen that the drainage effect of the drainage network depends on the longitudinal cross-sectional area of the drainage network. The larger the section of the drainage network, the smaller the corrosion of structural steel bars and buried metal pipelines [26]. Because the longitudinal resistance of the drainage network decreases due to the increase in the cross-sectional area, the effect of drainage has been significantly improved.

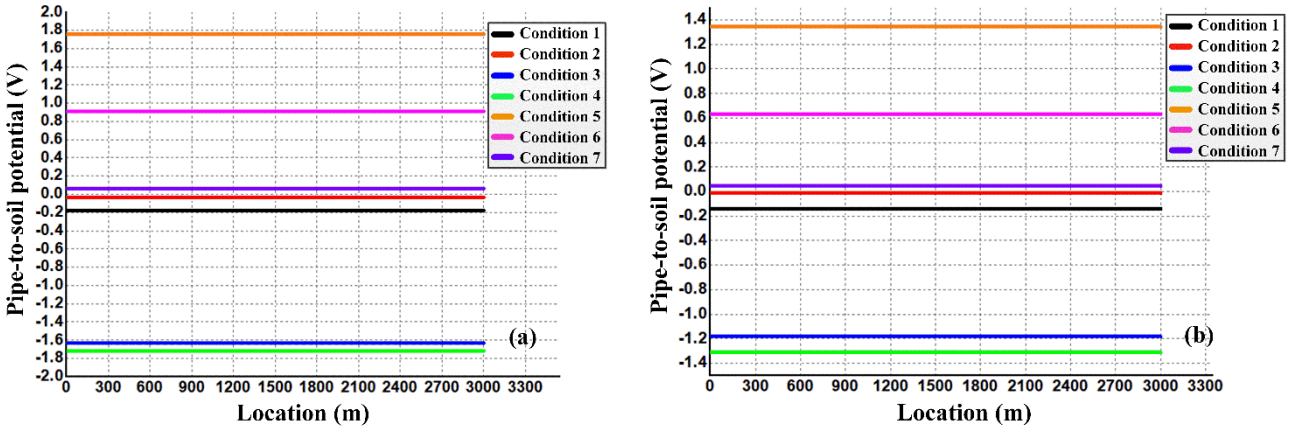

Figure 8. The ground potential of the buried pipeline in the length direction: (a) uncommitted and (b) committed

5.2 Protective effect of insulation and anticorrosion coating for buried pipeline

The electrochemical reaction between the buried pipeline metal and soil electrolytes is the main cause of buried pipeline corrosion. To avoid the occurrence of buried metal corrosion, the most effective way is to block the electrochemical reaction [27-28]. In pipeline corrosion prevention and control work, by adding an anti-corrosion layer on the outer surface of the pipeline, stray currents can be effectively prevented from entering the metal layer of the pipeline, thereby achieving corrosion prevention and control. There are three commonly used anticorrosive coatings in China: three-layer polyethylene (3PE), epoxy powder and petroleum bitumen[29-30]. The parameters are shown in Table 1.

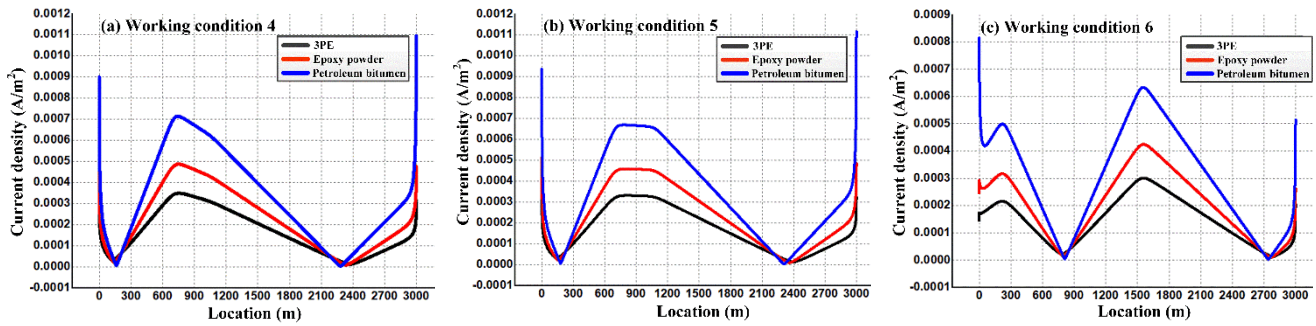

Figure 9. Protective effect of buried pipeline anticorrosion layer: (a) working condition 4, (b) working condition 5, and (c) working condition 6.

Fig. 9 shows the current density curve on the pipeline under three different anticorrosive layers, operations 4, 5 and 6. It can be clearly seen that the distribution trend of stray current on buried pipelines is the same at the same time. The peak position of the curve in the middle of the pipeline is where the train is located, so the current density is higher. At both ends of the pipe is the location where the current flows out, so the current density is higher. As far as the protective effect is concerned, it can be found that 3PE has the best protective effect, followed by epoxy powder and petroleum bitumen antiseptic layer. However, even for petroleum asphalt anti-corrosion layer, the current density decreases from 0.1 A/m^2 without anti-corrosion layer to 0.00072 A/m^2 at working condition 4, from 0.105 A/m^2 to 0.00063 A/m^2 at working condition 6, and the protection efficiency of stray current is 99.3% and 99.4%, respectively. Compared with Zhou's conclusion [31] of 3PE 90% protection efficiency, the anti-corrosion efficiency of this paper is higher. Therefore, for buried pipelines near Metro lines, the setting of the anticorrosive layer can effectively reduce the corrosion of stray current. During the laying of buried pipelines along Metro lines, the setting of the anticorrosive layer should be widely popularized.

6. CONCLUSION

The distribution of stray current in the subway is the result of the common influence of multiple parameters. In this paper, a resistance network model and an electric field model are combined to form a field-circuit coupling model. Under the actual operation condition of the train, the interference of stray current on buried pipelines is analyzed to provide analysis methods for engineering practice and theoretical guidance for stray current protection of buried pipelines. The following conclusions are drawn in this paper.

(1) The train runs periodically in the subway power supply section, and the leakage law of stray current in the section will also appear periodically with the traction motion of the train. The magnitude and location of the stray current leakage are directly affected by the train position and traction current.

(2) The field-circuit coupling model that combines a resistance network model and an electric field model simplifies the calculation process and can specifically analyze the trend of the corrosion area of the buried pipeline under the interference of stray current. The simulation results show that the interference degree of stray current to the pipeline does not depend entirely on the number of trains on the line but on the average traction current of the train. In the periodically changing catenary power supply interval, the area from 500 m to 2000 m of the buried pipeline is the key area of stray current interference, so the corrosion protection in this area should be strengthened.

(3) The input of the drainage network can reduce the leakage of stray current. The longitudinal resistance of the drainage network determines the collection effect of stray current. Setting of an anti-corrosion layer can greatly reduce the interference of stray current on buried pipelines. The simulation results show that the protective efficiency of 3PE, epoxy powder and petroleum bitumen against stray current can be more than 90%. The specific protective layers can be selected according to the protection requirements in practical projects.

ACKNOWLEDGEMENT
This work was supported in part by the Natural Science Foundation of China under Grant 51807065, in part by the Key Research and Development Plan of Jiangxi Province under Grant 20202BBEL53015.

CONFLICTS OF INTEREST
The authors declare no conflict of interest.

References

1. K.K. Tang, *Cem. Concr. Res.,* 100 (2017) 445.
2. L. Bertolini, M. Carsana, P. Pedeferri, *Corros. Sci.*, 49 (2007) 1056.
3. A. Mujezinović and S. Martinez, *IEEE Trans. Power Delivery,* 36 (2021) 1015.
4. L.H. Mu, W.Z. Shi and M.R. Zhang, *J. China Rail. Soc.*, 29 (2007) 45.
5. B. Mccollum and G.H. Ahlborn, *J. Franklin Inst.,* 1 (1916) 108.
6. X.H. Wang, C.X. Qiang,C.Y. Tu,Y.C. Chen and Y.C. Li, *Int. J. Electrochem. Sci.*, 12 (2017) 6520.
7. S.Y. Xu, W. Li and Y.Q. Wang, *IEEE Trans. Veh. Technol.*, 62(2013) 3569.
8. A. Ogunsola, L. Sandrolini and A. Mariscotti, *IEEE Trans. Ind. Appl.*, 51 (2015) 5431.
9. Y.J. Hu, Z. Zhong and J.P. Fang, *China Railway Sci.*, 32 (2011) 129.
10. Y. Hong, Z.H. Li, G.F. Qiao and J.P. Ou, *Constr. Build. Mater.*, 157 (2017) 416.
11. L. Bortels, A. Dorochenko, B. Van den Bossche, G. Weyns and J. Deconinck, *Corros.*, 63 (2007) 561.
12. J. Geng, Q.J. Ding and Q.J. Ding, *Int. J. Electrochem. Sci.*, 13 (2018) 6098.
13. Y.Q. Wang, W. Li, S.Y. Xu and X.F. Yang, *Int. J. Electrochem. Sci.*, 8 (2013) 5314.
14. C.T. Wang, W. Li, Y.Q. Wang, X.F. Yang and S.Y. Xu, *Constr. Build. Mater.*, 247 (2020) 118562.
15. C.T. Wang, W. Li, Y.Q. Wang and K.P. Li, *Energ.*, 12 (2019) 746.
16. C. Cheng, Q.L. Zhao, Z.L. Ma and T. Yao, *IEEE Access*, 8 (2020) 35973.
17. W. Liu, F.Q, Li, J.S. Tang, L. He, G.Y. Sang and K.P. Li, *High Voltage Appar.*, 46 (2020) 2856.
18. A.M. Wang, S. Lin, J.Y. Li and Z.Y. He, *High Voltage Appar.*, 46 (2020) 1379.
19. G.F. Du, J. Wang, Z.K. Zhu, Y.H. Hu and D.L. Zhang, *IEEE Trans. Transp. Electrif.*, 5 (2019) 490.
20. F. Zhu, J.C. Li, H.B. Zeng and R.Q. Qiu, *High Voltage Eng.*, 44 (2018) 2738.
21. L. Fan, X. Tan, Q.H. Zhang, W.N. Meng, G.D. Chen and Y. Bao, *Eng. Struct.*, 204 (2020) 110039.
22. A. Zaboli, B. Vahidi, S. Yousefi, M. M. Hosseini-Biyouki, IEEE Trans. Veh. Technol., 66 (2017) 974.
23. D.L. Ma, J.M. Fang and Y.H. Qian, *J. Mech. Electr. Eng.,* 34(2017)1465.
24. C. Li, J.G. Wang, Y.D. Fan, M. Zhou, M.R. Gong and S.W. Liu, *High Voltage Eng.*, 41 (2015) 3604.
25. H. Jin and S. Yu, *Constr. Build. Mater.,* 272 (2021).
26. C.T. Wang, W. Li, Y.Q. Wang, S.Y. Xu and M.B. Fan, *Int. J. Electrochem. Sci.,* 13 (2018) 1700
27. H.W. Huang, X.X. Sheng, Y.Q. Tian, L. Zhang, Y. Chen and X.Y. Zhang, *Ind. Eng. Chem. Res.*, 59 (2020) 15424.
28. Y.C. Chen, X.H. Wang, Y.C. Li, G.Z. Zheng and X.Y. Tu, *Int. J. Electrochem. Sci.,* 11 (2016) 10884.
29. X. Wang, C. Wang, X. Tang and Z. Guo, *Int. J. Electrochem. Sci.,* 9 (2014) 7660.
30. Y.P. Perelygin, A.E. Rosen, I.S. Los' and S.Y. Kireev, *Prot. Met. Phys. Chem. Surf.*, 50 (2014) 856.
31. S.Y. Zhou, X. Wang, Y.L. Chu, H.P. Liu and D.T. Sun, *Weld. Pipe Tube,* 44 (2021) 55.